ARTICLE

TNF-α impairs EP4 signaling through the association of TRAF2-GRK2 in primary fibroblast-like synoviocytes

Yu Tai[1], Bei Huang[1,2], Pai-pai Guo[1], Zhen Wang[1], Zheng-wei Zhou[1], Man-man Wang[1], Han-fei Sun[1], Yong Hu[3], Sheng-lin Xu[3], Ling-ling Zhang[1], Qing-tong Wang[1] and Wei Wei[1]

Our previous study showed that chronic treatment with tumor necrosis factor-α (TNF-α) decreased cAMP concentration in fibroblast-like synoviocytes (FLSs) of collagen-induced arthritis (CIA) rats. In this study we investigated how TNF-α impairs cAMP homeostasis, particularly clarifying the potential downstream molecules of TNF-α and prostaglandin receptor 4 (EP4) signaling that would interact with each other. Using a cAMP FRET biosensor PM-ICUE3, we demonstrated that TNF-α (20 ng/mL) blocked ONO-4819-triggered EP4 signaling, but not Butaprost-triggered EP2 signaling in normal rat FLSs. We showed that TNF-α (0.02–20 ng/mL) dose-dependently reduced EP4 membrane distribution in normal rat FLS. TNF-α significantly increased TNF receptor 2 (TNFR2) expression and stimulated proliferation in human FLS (hFLS) via ecruiting TNF receptor-associated factor 2 (TRAF2) to cell membrane. More interestingly, we revealed that TRAF2 interacted with G protein-coupled receptor kinase (GRK2) in the cytoplasm of primary hFLS and helped to bring GRK2 to cell membrane in response of TNF-α stimulation, the complex of TRAF2 and GRK2 then separated on the membrane, and translocated GRK2 induced the desensitization and internalization of EP4, leading to reduced production of intracellular cAMP. Silencing of TRAF2 by siRNA substantially diminished TRAF2-GRK2 interaction, blocked the translocation of GRK2, and resulted in upregulated expression of membrane EP4 and intracellular cAMP. In CIA rats, administration of paroxetine to inhibit GRK2 effectively improved the symptoms and clinic parameters with significantly reduced joint synovium inflammation and bone destruction. These results elucidate a novel form of cross-talk between TNFR (a cytokine receptor) and EP4 (a typical G protein-coupled receptor) signaling pathways. The interaction between TRAF2 and GRK2 may become a potential new drug target for the treatment of inflammatory diseases.

Keywords: rheumatoid arthritis; fibroblast-like synoviocytes; TNFR2; TRAF2; GRK2; EP4

Acta Pharmacologica Sinica (2022) 43:401–416; https://doi.org/10.1038/s41401-021-00654-z

INTRODUCTION

Fibroblast-like synoviocyte (FLS) hyperplasia is the principle feature and initiator of rheumatoid arthritis (RA). Excessive proliferation of FLSs is triggered by a variety of proinflammatory cytokines, including tumor necrosis factor-α (TNF-α), interleukin 1β (IL-1β) and prostaglandin E_2 (PGE$_2$) [1]. TNF-α is a major mediator of the inflammatory response and is implicated in the onset of RA [2]. In addition, TNF-α significantly promotes the production of PGE$_2$ in FLSs [1]. Cytokine-mediated induction of PGE$_2$ is the key factor that induces arthralgia both locally and centrally; furthermore, PGE$_2$ was reported to be a major player in exacerbating the proliferation of synoviocytes [3]. These pathological functions of PGE$_2$ clearly illustrate the beneficial effects of selective cyclooxygenase-2 (COX-2) inhibitors and nonsteroidal anti-inflammatory drugs (NSAIDs) in the clinic. Both types of anti-inflammatory drugs exert their functions mainly through inhibiting COX, thus impairing the production of PGE$_2$ [4, 5].

Conversely, a potent immunosuppressive or immunomodulatory effect of PGE$_2$ was reported based on its ability to increase intracellular cAMP levels [6, 7]. PGE$_2$ binds and activates four prostaglandin receptors (EPs), known as EP1, EP2, EP3 and EP4 [8], which are typical G protein-coupled receptors (GPCRs) and are precisely controlled by G protein-coupled receptor kinases (GRKs) and β-arrestins. EP2 and EP4 are linked to stimulatory G protein (Gαs), through which they activate adenylate cyclase (AC) and increase intracellular cyclic adenosine monophosphate (cAMP) levels; EP1 is linked to Gαq, while EP3 couples with inhibitory G protein (Gαi) and reduces cAMP levels [9]. Human FLSs (hFLSs) have constitutive mRNA expression of EP2 and EP4; however, there have been inconsistent reports on EP1 and EP3 mRNA expression [10]. Therefore, EP2 and EP4 are regarded as attractive pharmacological targets for RA treatment. In the inflammatory microenvironment of arthritic joints, abundant PGE$_2$ stimulation leads to increases in intracellular cAMP levels via the activation of EP2 and EP4, thus inhibiting FLS proliferation through the following pathways: (a) activating exchange protein activated by cAMP (EPAC)/Rap1 signaling [11]; (b) inhibiting extracellular signal-regulated kinase (Erk) phosphorylation and the mitogen-

activated protein kinase (MAPK) pathway, which controls cell proliferation and differentiation [12]; (c) promoting the inhibitory effect of C1q/TNF-related protein (CTRP) 9 on DNA synthesis [13]; (d) suppressing the activation of mammalian target of rapamycin complex (mTORC) by both PKA and the PKB-MAPK/adenosine monophosphate activated protein kinase (AMPK)-TSC1/2 pathway, thus triggering the dissociation of mTORC and the inactivation of mTOR kinase, which leads to the inhibition of cell proliferation [14]; and e) controlling the transcription of proliferative genes targeted by cAMP element binding (CREB) or the YAP ortholog Yorki [15]. The fundamental underlying reason for opposing functions of PGE_2-EP signaling in the inflammatory microenvironment with abnormal increases in the proinflammatory cytokine TNF-α is worth exploring to attain better understanding of the pathogenesis of RA. Moreover, how TNF-α affects EP receptor-mediated signaling remains largely unknown.

TNF-α interacts with two different receptors: TNF receptor 1 (TNFR1) and TNFR2. TNFR family signaling is mediated by tumor necrosis factor receptor-associated factors (TRAFs). To date, six TRAF family proteins (TRAF1-TRAF6) have been identified. All TRAFs share a common sequence of amino acids at their carboxyl termini termed the TRAF domain, which is required for the binding of the cytoplasmic domain [16].

Typically, TNFR signaling is independent of the cAMP pathway, but interestingly, our previous work showed that after TNF-α stimulation, the cAMP concentration in FLSs in collagen-induced arthritis (CIA) rats was decreased [17]. The present study aimed to explore how TNF-α regulated cAMP production in FLSs, particularly by further clarifying the potential downstream molecules of TNF-α and EP4 signaling that interact with each other. This investigation will not only identify a new form of crosstalk between TNF-α and EP4 signaling but also reveal a novel pattern of TNF-α action in inflammatory arthritis.

MATERIALS AND METHODS

Experimental animals
Sprague–Dawley (SD) rats (male, 140 ± 20 g, Certificate No. SCXK (WAN) 2011–002) were obtained from the Animal Department of Anhui Medical University (Hefei, China). All rats were maintained under SPF conditions. The experiments reported here were approved by the Ethics Review Committee for Animal Experimentation of the Institute of Clinical Pharmacology, Anhui Medical University.

Antibodies and reagents
Incomplete Freund's adjuvant (IFA) and chick CB peptides of type II collagen (CII) were obtained from Chondrex Inc. (Redmond, WA, USA). Recombinant human TNF-α was purchased from Peprotech Inc. (Rocky Hill, NJ, USA). Indometacin (Cat. No. 17378) was obtained from Sigma-Aldrich (Saint Louis, MO, USA). TNF-R1 (H-5) (Cat#: sc-8436), TNF-R2 (D-2) (Cat#: sc-8041), EP4 (Cat#: sc-55596), GRK2 (C-9) (Cat#: sc-13143), TRAF2 (H-10) (Cat#: sc-7346), TNFR1 siRNA (siTNFR1) (Cat. No. sc-29507), TNFR2 siRNA (siTNFR2) (Cat. No. sc-36689), and control siRNA (Cat. No. sc-37007) were purchased from Santa Cruz Biotechnology (Dallas, TX, USA). Protein A+G (Cat. No. P2012) agarose was obtained from Beyotime (Shanghai, China). Cy3-conjugated Goat anti-mouse IgG (H+L) (Cat#: 115–167–003), Alexa Fluor 488 AffiniPure goat anti-mouse IgG (H+L) (Cat#: 115–545–062), Alexa Fluor Rhodamine Red AffiniPure donkey anti-goat IgG (H+L) (Cat#: 705–295–003) and Alexa Fluor 488 AffiniPure goat anti-rabbit IgG (H+L) (Cat#: 111–005–003) antibodies were purchased from Jackson ImmunoResearch Inc. (West Grove, PA, USA). The Gαs activation assay kit (Cat. No. 80801) was purchased from New East Biosciences (King of Prussia, PA, USA). The ^{125}I-cAMP radioimmunoassay (RIA) kit was obtained from the Nuclear Medicine Laboratory of Shanghai College (Shanghai, China). An enzyme-linked immunosorbent assay (ELISA) kit for PGE_2 was purchased from Research & Development Co., Ltd. (MN, USA). Phospho-GRK2 (pSer670) was obtained from Pierce Biotechnology (Rockford, IL, USA). A Lipofectamine 2000 transfection kit from Invitrogen (Carlsbad, CA, USA) was used as suggested by the supplier. The SuperScript First-Strand Synthesis System for RT-PCR kit (Cat. No. 11904–018) was purchased from Invitrogen (Carlsbad, CA, USA). The primers for EP4, TRAF2 and GAPDH were obtained from Invitrogen (Shanghai, China). TRAF2 and control small interfering RNA (siRNA) were synthesized by Invitrogen (Shanghai, China). The control sequence does not match any human genome sequence.

Induction of CIA
CIA was induced by immunizing rats with native chicken CII that had been dissolved overnight at 4 °C in 0.1 M acetic acid (2 mg/mL) and emulsified with an equal volume of IFA. Rats were injected with 0.2 mL (collagen: 200 mg) of the emulsion subcutaneously at the base of the tail. A booster injection was given on day 7 after the initial immunization. Control rats were injected with vehicle. The day of the first immunization was defined as day 0.

In vivo drug administration
After the onset of CIA (around 14d), model rats were randomly divided into CIA-Veh, CIA-MTX and CIA-Paroxetine groups according to the clinical scores. MTX (0.5 mg/kg every 3 days) and paroxetine (15 mg·kg^{-1}·d^{-1}) were dissolved in 0.5% CMC-Na and administered by gavage for 15 days.

Arthritis assessment
Rats were inspected daily for signs of arthritis by two independent observers who were not aware of the treatments. The uninjected hind paw volume was measured with a YLS-7B toe volume meter. Paw swelling (△mL) was calculated by subtracting the paw volume at day 0. The arthritis severity of each paw was evaluated by using a macroscopic scoring system ranging from 0 to 4 (0, paws with no swelling or focal redness; 1, mild but definite redness and swelling of the ankle or wrist or apparent redness and swelling limited to individual digits, regardless of the number of affected digits; 2, moderate redness and swelling of the ankle or wrist; 3, severe redness and swelling of the entire paw, including digits; and 4, maximally inflamed limbs with the involvement of multiple joints). The cumulative score for all four paws of each mouse was used as the polyarthritis index and had a maximum value of 16 [18].

Histopathological joint examination
The hind paws of rats were removed on day 28, fixed with neutral buffered 10% formalin, decalcified for 10 days with EDTA and embedded in paraffin for histological analysis. The paraffin sections were stained with hematoxylin and eosin. The micrographs were evaluated histologically by two independent observers.

The severity of arthritis in the joint was graded from 0 to 4 according to the intensity of lining layer hyperplasia, mononuclear cell infiltration, and pannus formation (grade 0, normal ankle joint; grade 1, normal synovium with occasional mononuclear cells; grade 2, definite arthritis with a few layers of flat to rounded synovial lining cells, scattered mononuclear cells and dense infiltration of mononuclear cells; grade 3, clear hyperplasia of the synovium with three or more layers of loosely arranged lining cells and dense infiltration of mononuclear cells; and grade 4, severe synovitis with pannus formation and erosions of articular cartilage and subchondral bone) [19].

FLS culture
Rat FLSs were obtained from the joint synovia of normal SD rats or CIA rats as specified. Normal hFLSs were isolated from primary

synovial tissue obtained from trauma patients who had undergone total joint replacement surgery or synovectomy, and RA hFLSs were isolated from primary synovial tissue obtained from RA patients as indicated [20]. Informed consent was obtained from all patients, and the study protocol was approved by the Anhui Medical University Ethics Committee. FLSs were grown in DMEM with 10% fetal bovine serum (FBS) at 37 °C in a humidified atmosphere of 5% CO_2. Passage 3–8 cells were used for subsequent experiments.

FRET analysis of cAMP

YFP/CFP PM-ICUE3 adenovirus was added to the culture medium of rat FLSs, which was changed to fresh complete medium 4 h later. Forty-eight hours after infection, cells coexpressing the cAMP sensor (ICUE) were plated in imaging dishes and imaged in the dark at 37 °C on a temperature-controlled stage using a Leica DM IRB (Leica Microsystems) microscope with a CoolSnap Fx cooled charge-coupled device camera (Ropper Scientific) controlled by MetaFluor 7.5 (Universal Imaging Corporation, Downingtown, PA, USA). Dual emission ratio imaging was carried out using a 436DF10 excitation filter, a 436–510 DBDR dichroic mirror, and 480-AF30 and 550-AF30 emission filters for CFP and YFP, respectively. The exposure time was 200 ms, and images were taken every 20 s. Typically, equal sensor-positive cells and nonspecific areas were chosen in the microscopic field. The development of fluorescence was recorded individually in each area for the duration of the experiment. Several independent plates were analyzed according to this procedure, and the specific FRET signals of each cell (positive minus negative area) were pooled. Cells displaying a range of intensities were selected and analyzed without any impact of the sensor expression level on the responsiveness noted. After 5 min of baseline measurement, cells were stimulated with 20 ng/mL TNF-α, the control group was not stimulated, and 1 μM PGE$_2$, Butaprost or ONO-4819 was added as a positive control after 20 min of stimulation. A low hormone dose was chosen to avoid saturation of the ICUE sensor, which has a limited dynamic range compared to that of BRET assays. The fluorescence intensity of nonspecific areas was subtracted from the intensity of fluorescent cells expressing the sensor to quantify the specific signal. The FRET ratio (CFP/YFP) was calculated for each individual cell. The data represent the mean ± SEM of at least 20 individual cell responses measured in three independent experiments.

Flow cytometric analysis

FLSs were detached with 1 mM PBS EDTA, fixed with 4% paraformaldehyde, and then suspended in fluorescence-activated cell sorting (FACS) buffer (PBS/0.1% bovine serum albumin/0.01% NaN$_3$). A total of 1×10^5 cells were incubated with specific primary antibodies overnight at 4 °C and then incubated for 2 h with the corresponding fluorescently labeled secondary antibodies. As a negative control, FLSs were incubated with fluorescently labeled secondary antibodies only. Cells were then washed, resuspended in FACS buffer and analyzed by flow cytometry (FC500, Beckman). Data analysis was performed using Cell Quest™ analysis software.

Determination of hFLS viability

To test the effect of TNF-α on hFLS proliferation, hFLSs were seeded in triplicate in a 96-well plate at 1.5×10^4 cells/well and cultured for 6 h. The cells were then treated with TNF-α (20 ng/mL) or TNF-α + INN (20 ng/mL + 1×10^{-6} M) for 48 h. The number of metabolically active mitochondria and viable cells was determined at 490 nm using the 3-(4,5-dimethylthiazol-2-yl)-2,5-diphenyltetrazolium bromide (MTT) assay.

Measurement of cAMP concentrations

After the indicated treatments in 24-well plates, cell culture supernatants were discarded, and hFLSs (5×10^4 cells/well) were washed with ice-cold PBS. The cells were then dissociated in lysis buffer and centrifuged at $1500 \times g$ for 3 min at 4 °C, and the supernatants were immediately frozen for later use. The concentration of intracellular cAMP was measured using a ^{125}I-cAMP RIA kit according to the instructions specified by the manufacturer [21].

Protein extraction and membrane preparation

To prepare total cell lysates, FLSs (1×10^5 cells/well) in 6-well plates were washed with ice-cold PBS and lysed in ice-cold lysis buffer containing 50 mM Tris, 150 mM NaCl, 1% Nonidet P-40, and protease inhibitor cocktail (Sigma-Aldrich) for 40–50 min at 4 °C. The lysates were centrifuged for 4 min at 3000 rpm, and the resulting supernatants were diluted to 1 mg protein/mL and kept frozen at −80 °C to analyze total protein expression. Membrane fragments were obtained from the supernatant by centrifugation at $30,000 \times g$ for 2.5 h, and the pellet was resuspended in PBS [22]. The efficiency of protein extraction was determined using pan-cadherin, a general plasma membrane marker, as described previously [23]. The protein content was determined by standard bovine serum albumin protein assays.

Coimmunoprecipitation

FLSs were lysed in 0.5 mL of lysis buffer and centrifuged for 10 min at $10,000 \times g$ in a refrigerated centrifuge. The supernatant was collected, mixed with 5× Laemmli buffer, and then boiled for 5 min. The whole-cell lysate was precleared for 30 min at 4 °C with 20 μL of protein A+G agarose. The precleared cell lysates were subsequently incubated with 2 μg of the primary antibody for 1 h, 20 μL of protein A+G agarose beads was added, and the incubation was continued overnight at 4 °C with constant rotation. Next, the agarose beads were pelleted by centrifugation at 2500 rpm for 5 min at 4 °C. After extensive washes with ice-cold lysis buffer, the beads were resuspended in sample loading buffer, boiled for 5 min, and subjected to SDS-polyacrylamide gel electrophoresis, and the interaction of both proteins was detected by the corresponding primary antibody [24].

Western blotting

Proteins were separated by SDS-PAGE, electroblotted onto PVDF membranes (Bio-Rad), blocked for 2 h in 5% nonfat milk in TBS-0.1% Tween and incubated with the indicated primary antibodies diluted 1:1,000 in primary antibody dilution buffer (Beyotime, China) and the appropriate secondary antibody diluted 1:10,000 in 5% nonfat milk in TBS-0.1% Tween. Autoradiographs were detected using a LAS400Mini Chemilux CCD camera (GE Healthcare). All the experiments reported in this study were performed three times, and the results were reproducible.

Laser confocal microscopy

Immunofluorescence analysis was performed as described previously [25]. Briefly, hFLSs were seeded in chamber slides, fixed in 4% paraformaldehyde at room temperature, permeabilized with 0.2% Triton X-100, blocked with 1% BSA at 37 °C for 0.5 h in a humidified chamber, incubated with anti-TNFR1, anti-TNFR2, anti-TRAF2, or anti-GRK2 overnight at 4 °C, washed with PBS three times, and then incubated with Alexa Fluor 488-conjugated or Cy3-conjugated secondary antibodies (Invitrogen) at 37 °C for 2 h. Following three washes in PBS, DNA was counterstained with DAPI for 5 min. Fluorescent images were collected under a Leica SP5 laser scanning confocal microscope. The gray value per pixel was measured by the plot profile function of ImageJ software. The area under the curve (AUC) was used to compare the fluorescence intensity, including protein expression and distribution on the cell membrane and in the cytoplasm and total cells. The average relative fluorescence intensity (AFI) of protein expression in total cells was quantified using ImageJ software (version 1.42q, NIH).

404

High content screening

hFLSs were seeded in 96-well plates, fixed in 4% paraformaldehyde at room temperature, permeabilized with 0.2% Triton X-100, blocked with 1% BSA at 37 °C for 0.5 h in a humidified chamber, washed with PBS three times, and counterstained with DAPI for 5 min. Fluorescent images were taken under a mage Xpress Micro 4 high content screening system.

Small interfering RNA transfection

Before transfection, hFLSs were cultured to 70%–80% confluence at 37 °C as described previously and then transfected with the siRNA using Lipofectamine 2000 transfection reagent according to the manufacturer's protocol. hFLSs were transiently transfected with 50 nmol of siRNA. The transfection efficiency was analyzed by RT-PCR or Western blotting after 24 h, and the maximum transfection efficiency of each siRNA was determined. The siRNA sequences were as follows: TRAF2 sense: 5'-AAUGCCGGCAGCU CAGGCUUCUCUC-3'; TRAF2 antisense: 5'-GAGAGAAGCCUGAG CUGCCGGCAU-3'; negative control sense: 5'-UUCUCCGAACGUGU CACGUTT-3'; and antisense: 5'-ACGUGACACGUUCGGAGAATT-3'.

Real-time qPCR

Total RNA was prepared using TRIzol reagent (Invitrogen, Carlsbad, CA, USA). First strand cDNA was synthesized from total RNA (1 μg) by reverse transcription (Fermentas). PCR products were analyzed on a 1.5% agarose gel and stained with ethidium bromide for UV detection. Real-time PCR assays were performed with an Applied Biosystems 7500 fast real-time PCR system (ABI) using SYBR$^{®}$ green real-time PCR master mixe (Invitrogen). The oligonucleotide primer sequences were as follows: EP4 forward primer, 5'-AAGTCGCGCAAGGAGCAGAA-3'; EP4 reverse primer, 5'-CTTGTC CACGTAGTGGCTGT-3' (270 bp); TRAF2 forward primer, 5'-AGATT GAAGCCCTGAGTAGCAAGG-3'; TRAF2 reverse primer, 5'-ATCACCA CAAAGAAGAGGGACAGG-3' (304 bp); GAPDH forward primer, 5' -A CCACAGTCCATGCATCAC-3'; and GAPDH reverse primer, 5'-TCCAC CACCCTGTTGCTGTA-3'. Quantitative analysis was performed using the ratio of the target gene to GAPDH. All results are representative of at least three experiments [26].

Molecular docking analysis

Potential binding sites of GRK2 and TRAF2 were calculated using Discovery Studio (DS, version 2020). The crystal structure of human GRK2 (PDB ID: IYM7) and the TRAF domain of human TRAF2 (PDB ID: 1CA4) were obtained from RCSB Protein Data Bank 1. DS protein-protein docking was used to identify the interaction between GRK2 and TRAF2 and the potential binding sites. The lower energy pose indicated that stronger binding occurred.

Statistical analysis

All data were analyzed by GraphPad Prism 7 statistical software and are expressed as the mean ± SEM. Differences between multiple groups were evaluated by either one-way ANOVA with Tukey's posttest or two-way ANOVA with Sidak's posttest. A t-test was used to compare differences between two groups. P values less than 0.05 were considered to be significant. Western blotting and RT-PCR were repeated at least three times for each sample, and the results were subjected to semiquantitative analysis to ensure maximal accuracy of the conclusions drawn from these data.

RESULTS

EP4 signaling is blocked in TNF-α-stimulated FLSs

We previously showed that after TNF-α stimulation, the cAMP concentration in FLSs in SD rats was decreased [17], and cAMP is the key molecule in GPCR signaling. Many proinflammatory cytokines, such as TNF-α, IL-1, PGE$_2$, IL-17, IL-6, and GM-CSF, and chemokines are abundant in RA patients regardless of therapy

[27]. PGE$_2$ is produced in response to proinflammatory cytokines and plays an important pathogenic role through its receptors [28]. Among these important factors, PGE$_2$ receptors (EPs) are GPCRs.

Accordingly, we investigated the mechanism by which TNF-α decreased cAMP expression in FLSs. FLSs, which were isolated from the synovia of rats, were cultured in vitro in the presence of TNF-α (at final concentrations of 0, 0.02, 0.2, 2, or 20 ng/mL) for 48 h, and then cAMP levels were analyzed. At concentrations of 2 or 20 ng/mL, TNF-α notably decreased the cAMP level in FLSs (Fig. 1a). Rat FLSs were infected with adenovirus encoding PM-ICUE3, which is a cAMP fluorescence resonance energy transfer (FRET) biosensor anchored on the plasma membrane. PGE$_2$ (1 μM) induced abundant cAMP production in FLSs; however, PGE$_2$ signaling was attenuated by TNF-α (20 ng/mL) pretreatment for 48 h. Since the PGE$_2$ receptors EP2 and EP4 have been reported to be expressed on FLSs, we used specific EP2 and EP4 agonists to determine which receptor subtype was affected by TNF-α. Both the EP2 agonist butaprost and the EP4 agonist ONO-4819 triggered cAMP production in rat FLSs; notably, ONO-4819-induced cAMP signaling was significantly reduced by TNF-α pretreatment (Fig. 1b), indicating that EP4 function was blocked by chronic TNF-α stimulation. We then analyzed changes in the membrane expression of EP2 and EP4 in response to TNF-α stimulation. In accordance with the FRET data, 48 h of treatment with increasing concentrations of TNF-α decreased the membrane distribution of the EP4 subtype but not EP2 (Fig. 1c, d). A scatter plot of the membrane expression of EP4 and the concentration of TNF-α revealed a negative correlation (Fig. 1e) ($R^2 = -0.7805$, $P = 0.0469$). This correlation suggested that the membrane expression of EP4 was reduced upon TNF-α stimulation. Further analysis showed a significantly positive correlation between intracellular cAMP levels and EP4 membrane expression ($R^2 = 0.989$, $P = 0.0005$) (Fig. 1f). Since FLSs are able to produce PGE$_2$ under TNF-α stimulation, to eliminate the effect of endogenous PGE$_2$ on the receptors, indometacin (INN) was added to the system to inhibit PGE$_2$ synthesis. Induction with either TNF-α or TNF-α plus INN greatly decreased the membrane expression of EP4 but had no obvious effect on EP2 distribution. Consistent with the data reported, no expression of EP1 or EP3 was detected on the surface of rat FLSs by flow cytometry (Fig. 1g–i). These data indicate that TNF-α-induced downregulation of cAMP production is related to the internalization of EP4 in rat synoviocytes. In the following experiments, we confirmed this phenomenon in primary hFLSs and further investigated the potential mechanism of TNF-α-induced EP4 internalization in hFLSs. Analysis of the antibody-specific band showed that both total and cytoplasmic EP4 levels were elevated by TNF-α or TNF-α plus INN treatment (Fig. 1j, k). In contrast, membrane EP4 distribution was substantially reduced (Fig. 1l). As revealed by the present data, total and cytoplasmic EP4 expression was lower in the TNF-α plus INN group than in the TNF-α alone group, suggesting a role of PGE$_2$ in the response to TNF-α. It is known that EP4 couples with Gαs. Further research indicated that total Gαs expression was not notably changed under TNF-α or TNF-α plus INN stimulation (Fig. 1m). However, both treatments obviously decreased GTP-bound Gαs, which was activated. Interestingly, the activation of Gαs in hFLSs stimulated with TNF-α plus INN was higher than that in TNF-α-stimulated cells, suggesting that PGE$_2$ may attenuate the activation of Gαs (Fig. 1n). These data suggest that TNF-α directly induces EP4 receptor desensitization and internalization in FLSs.

TNF-α impairs EP4 signaling in hFLSs in a TNFR2-dependent manner

TNF-α is known to induce significant hFLS proliferation. The TNFR superfamily induces diverse biological effects, including cell survival, proliferation, differentiation, and apoptosis [29, 30]. In the present study, the membrane expression of TNFR1 and TNFR2 in hFLSs was examined by flow cytometry and Western blotting.
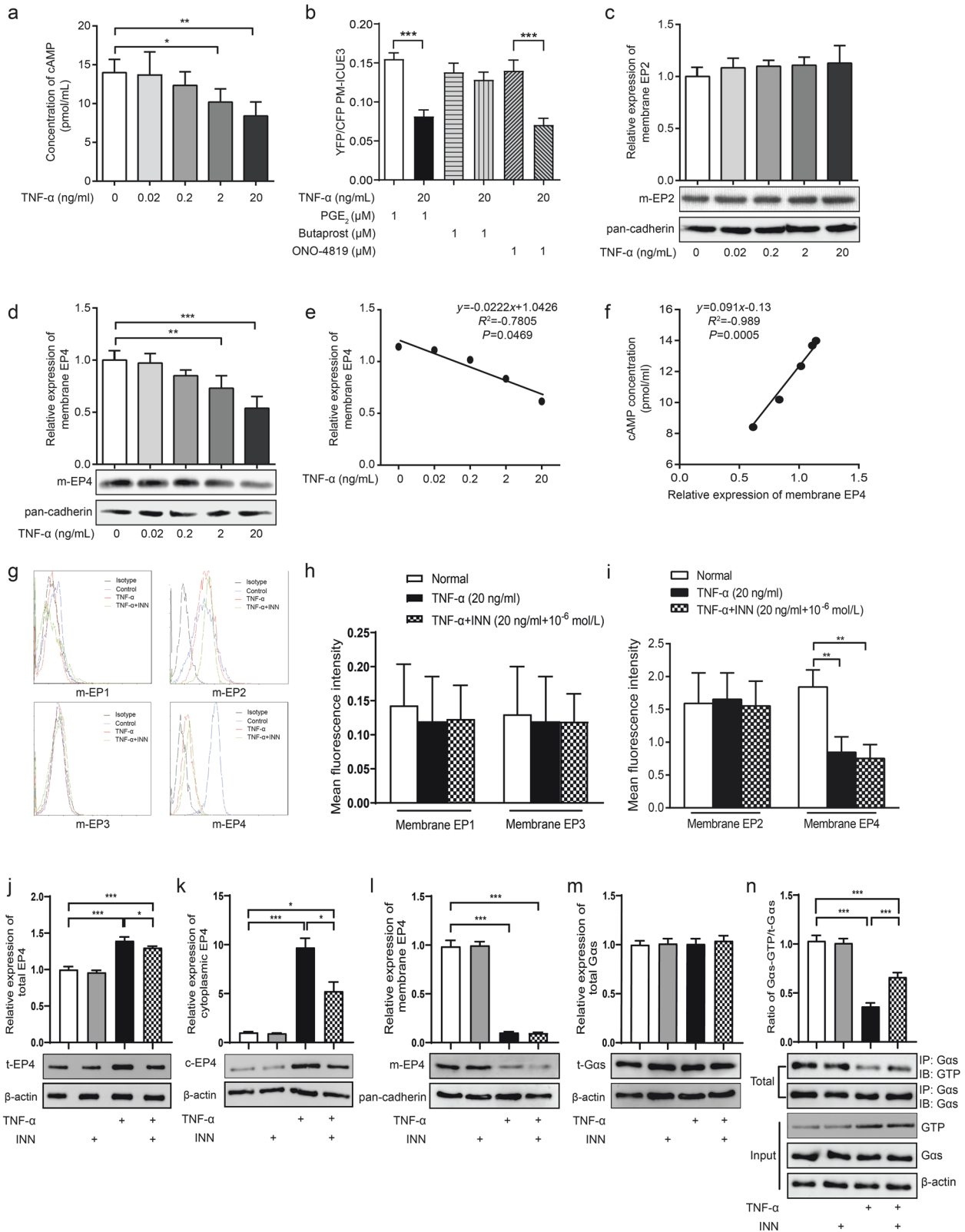
The results showed that membrane TNFR2 was obviously increased in response to TNF-α stimulation, but there was no significant change in TNFR1 expression (Fig. 2a–d). We silenced TNFR1 and TNFR2 gene expression by small interfering RNA (siRNA) transfection. The protein expression levels of TNFR1 and TNFR2 were measured by Western blotting to determine the optimal sequence. TNFR1 and TNFR2 protein expression in hFLSs was reduced by ~82.7% and 84.2%, respectively, in response to TNFR1- and TNFR2-specific siRNA compared with the negative control sequence (Fig. 2e, f). To determine which TNF-α receptor

Fig. 1 EP4 signaling is blocked in TNF-α-stimulated FLS. Normal FLSs were obtained from the synovia of SD rats or from trauma patients who had undergone total joint replacement surgery or synovectomy. **a** Rat FLSs were cultured in the presence of TNF-α at final concentrations of 0, 0.02, 0.2, 2, or 20 ng/mL for 48 h, and cAMP levels were analyzed by a ^{125}I-cAMP RIA kit. **b** Rat FLSs were transfected with a plasma membrane-linked cAMP biosensor, which has cyan fluorescent protein (CFP) and yellow fluorescent protein (YFP). Cyclic-AMP close to the plasma membrane binds to the EPAC1 domain of the PM-ICUE3 sensor and separates CFP and YFP, leading to a decrease in the intensity of the YFP/CFP ratio. **c**, **d** Rat FLSs were treated with different concentrations of TNF-α for 48 h, the cell membrane fraction was purified by centrifugation $30,000 \times g$, and EP2 and EP4 expression levels were determined by Western blotting. **e** The relationship between the exogenous TNF-α concentration and the relative membrane expression of EP4 was analyzed, and a negative association was observed. **f** A significant positive correlation between the relative membrane expression of EP4 and intracellular cAMP levels was described. **g–i** Rat FLSs were stained with primary EP1–4 antibodies and corresponding FITC-labeled secondary antibodies after treatment with vehicle, TNF-α 20 ng/mL, or 20 ng/mL TNF-α and 1 μM INN for 48 h; cells incubated with only the fluorescently labeled secondary antibody were used as an isotype control. Flow cytometry was used to observe the membrane expression of EP1–4 on FLSs, and the mean fluorescence intensities were compared between the different treatments. **j–l** Total, cytoplasmic and membrane levels of EP4 were measured in hFLSs treated with TNF-α (20 ng/mL) or TNF-α (20 ng/mL) and INN (1 μM) for 48 h. **m** Total Gαs expression was measured by Western blotting. **n** Coimmunoprecipitation was used to determine the level of activated GTP-bound Gαs. The ratio of Gαs-GTP to total Gαs was calculated to reflect the activation of Gαs. $*P < 0.05$, $**P < 0.01$, $***P < 0.001$ ($n = 6$).

subtype is involved in this process, we used siRNA to knock down TNFR1 or TNFR2 in hFLSs. High content screening was used to analyze hFLS proliferation in response to TNF-α stimulation. Under TNF-α stimulation, TNFR1-silenced hFLSs showed no changes in proliferation, but the proliferation of TNFR2-silenced hFLSs was reduced compared with that of normal hFLSs (Fig. 2g, h). Silencing TNFR2 but not TNFR1 decreased EP4 expression in response to TNF-α stimulation, as observed by laser confocal microscopy (Fig. 2i, j). The gray value per pixel was determined using the plot profile method. The AUC was used to compare the fluorescence intensity. These data suggest that TNF-α impairs EP4 signaling in hFLSs via TNFR2 but not TNFR1.

TNF-α impairs EP4 signaling in hFLSs in a TNFR2- and TRAF2-dependent manner

We designed the following experiments to confirm the role of TRAF2 in regulating EP4-cAMP signaling. The total protein expression of TRAF2 was significantly elevated by TNF-α stimulation compared with that in normal hFLSs, but TRAF2 expression was higher in hFLSs after stimulation with TNF-α plus INN than in those stimulated with TNF-α alone (Fig. 3a). In other words, TNF-α-induced PGE$_2$ diminished the expression of TRAF2. Evidence has shown that TRAF2 signaling is regulated by translocation. Recruitment of TRAF2 to plasma membrane lipid rafts is important for NF-κB signaling activation [31]. We then examined the expression of TRAF2 on the cell membrane. Consistent with the previous result, membrane TRAF2 expression was substantially increased upon stimulation by TNF-α plus INN or TNF-α alone, as detected by both Western blotting and laser confocal microscopy (Fig. 3b, c).

To determine the exact role of TRAF2, we silenced TRAF2 gene expression by siRNA transfection. The protein and gene expression levels of TRAF2 were measured by Western blotting and real-time qPCR, respectively, to determine the optimal sequence. TRAF2 gene expression was reduced by ~83.9%, while protein expression in hFLSs was reduced by ~89.9% in response to TRAF2-specific siRNA compared with the response to the negative control sequence (Fig. 3d). Subsequently, we found that TNF-α alone or in combination with INN obviously promoted hFLS viability. However, TNF-α alone increased cell viability compared with TNF-α plus INN administration. After TRAF2 knockdown, the effect of TNF-α plus INN on hFLS viability was significantly blocked (Fig. 3e). However, endogenous PGE$_2$ produced by hFLSs under TNF-α induction slightly promoted hFLS proliferation, suggesting that this effect may occur through a TRAF2-independent pathway. Thus, TRAF2 is clearly involved in TNF-α-induced hFLS proliferation.

The concentrations of cAMP were measured, and the results showed that in response to TNF-α alone or in combination with INN, intracellular cAMP levels were significantly decreased.

However, in TRAF2-defective hFLSs, TNF-α alone or in combination with INN failed to change the levels of cAMP (Fig. 3f), indicating that TRAF2 played a clear role in the TNF-α-induced decrease in cAMP production in hFLSs. Total and membrane EP4 protein levels were prominently increased; specifically, the level of membrane EP4 was much higher in response to TNF-α plus INN stimulation than in response to TNF-α stimulation alone. In TRAF2-silenced hFLSs, cytoplasmic EP4 expression was remarkably elevated in TNF-α-stimulated cells but was significantly decreased in cells induced by TNF-α plus INN (Fig. 3g–j), indicating that PGE$_2$ may slightly reduce EP4 membrane translocation. EP4 expression levels were determined by Western blotting and real-time qPCR and were prominently decreased by TRAF2 siRNA (Fig. 3k).

TNF-α triggered translocation of the TRAF2-GRK2 complex to the cell membrane and induced complex dissociation

TNFR2 is located on the cell membrane, and TRAFs have high TNFR2 binding capacities and are widely accepted to be common signal transducers for TNFR2. To explore how TNF-α promotes the desensitization of the EP4 receptor, we further tested whether TRAF2 interacts with GRK2/β-Arrestin2 using a coimmunoprecipitation assay. After stimulation with TNF-α or TNF-α plus INN, the interaction between TRAF2 and GRK2 was significantly diminished, as shown in Fig. 4a. Then, the distribution of the TRAF2-GRK2 complex was systematically examined. In primary hFLSs, the complex was principally located in the cytoplasm and hardly expressed on the cell membrane. TNF-α along or in combination with INN for 48 h significantly inhibited the association of TRAF2 and GRK2 in hFLSs (Fig. 4b, c), but the interaction between TRAF2 and β-arrestin2 did not change significantly (Fig. 4d).

Next, we found that GRK2 distinctly translocated to the cell membrane in response to both treatments (Fig. 4e), and there was a significant decrease in cytoplasmic GRK2 (Fig. 4f). Laser confocal microscopy revealed synchronous membrane translocation of both TRAF2 and GRK2 (Fig. 4g). To track the translocation of the TRAF2-GRK2 complex and capture the time point at which they dissociated under TNF-α stimulation, we examined the protein complex at different time points (0, 5, 10, 15, 30, and 60 min) in the cytoplasm and cell membrane. Figure 4h shows that the association of TRAF2 and GRK2 in the cytoplasm was reduced gradually after stimulation with TNF-α. The complex transferred to the cell membrane within 15 min, and then the two proteins separated from each other gradually, as detected at 30 and 60 min.

Next, we observed the interaction between these two proteins in vivo. TNF-α (20 ng/mL) was injected into the knee joint of normal SD rats. After 0, 5, 10, 15, 30, and 60 min, the synovium was collected, and then cytoplasm and membrane proteins were isolated. We noted that coimmunoprecipitation was increased in the cell membrane after treatment with TNF-α for 10 to 15 min
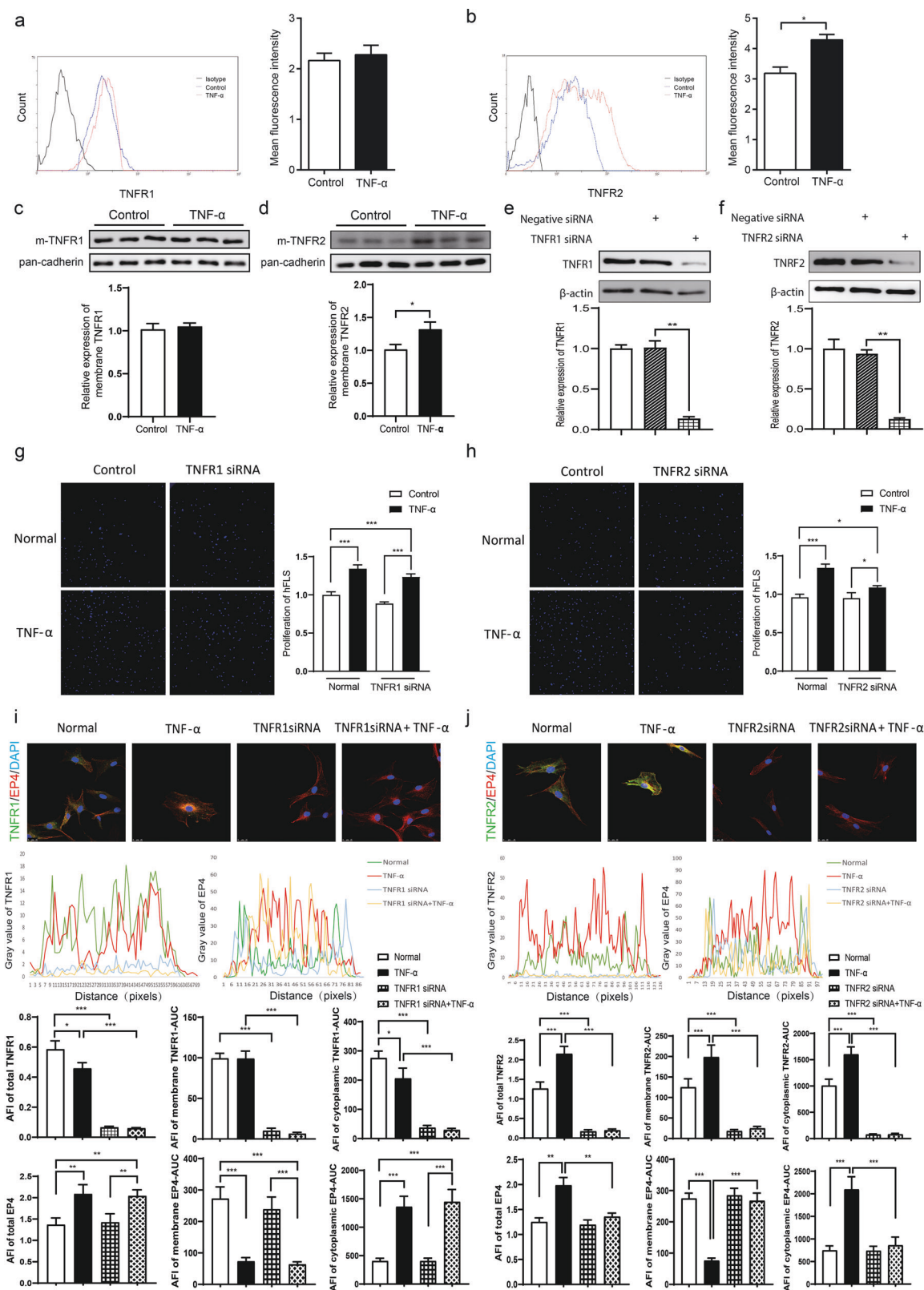
Fig. 2 TNF-α impairs EP4 signaling in hFLSs in a TNFR2-dependent manner. a, b TNFR1 and TNFR2 were indirectly stained with FITC-labeled secondary antibodies, and the distribution of these receptors was further observed using a laser confocal microscope. **c, d** The expression of membrane TNFR1 or TNFR2 on hFLSs was measured by Western blotting. **e, f** TNFR1 and TNFR2 gene expression was silenced by siRNA, and the protein expression of TNFR1 or TNFR2 was clearly downregulated. **g, h** High content screening was used to analyze hFLS proliferation (×100). **i, j** Laser confocal light microscopy was used to examine the expression of EP4 in hFLSs with or without TNFR1/2. *P < 0.05, **P < 0.01, ***P < 0.001 (n = 6).
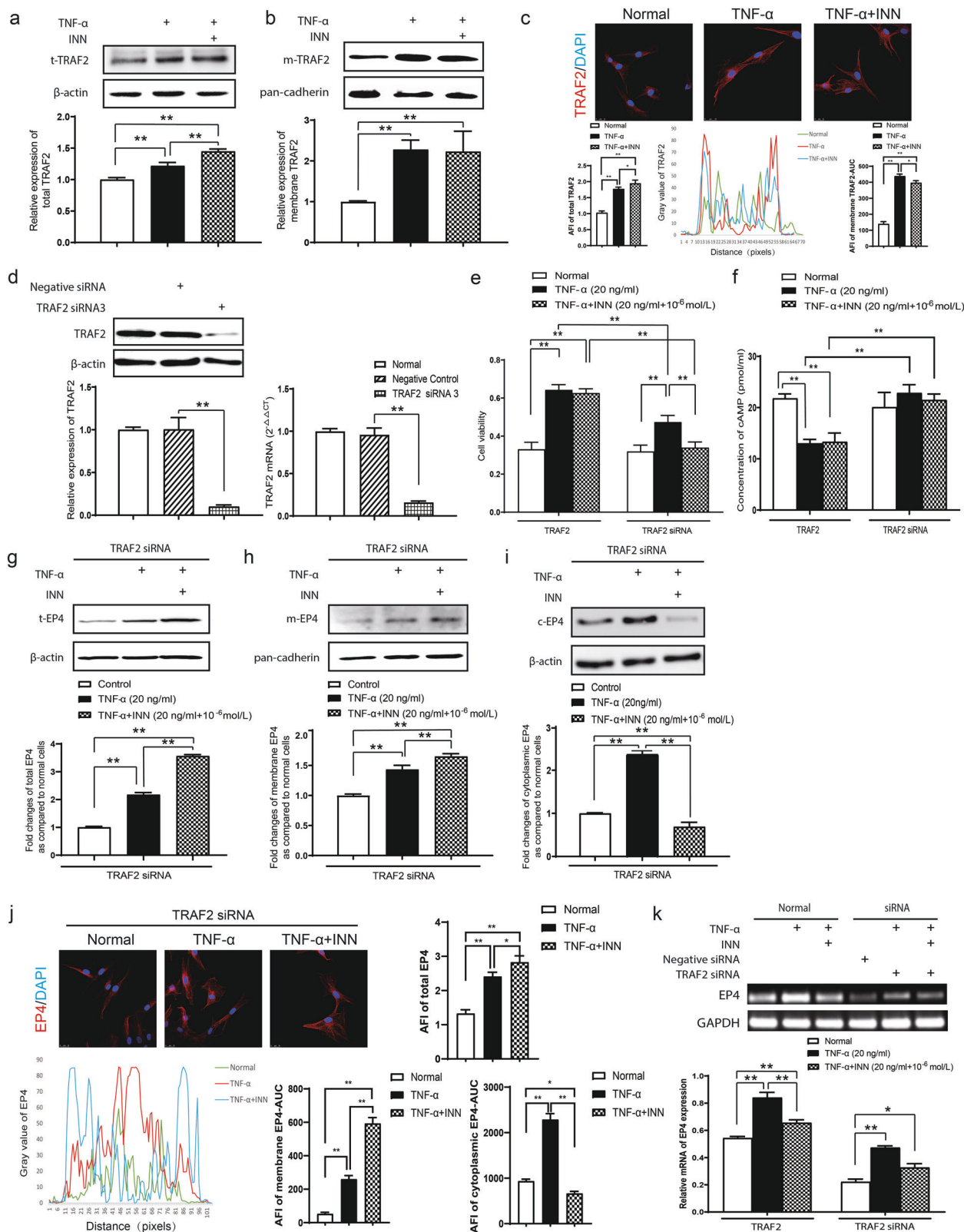
Fig. 3 TNF-α impairs EP4 signaling in hFLSs in a TNFR2- and TRAF2-dependent manner. a Total expression of TRAF2 was measured in hFLSs treated with TNF-α with or without INN. **b** Membrane TRAF2 was examined by Western blotting. **c** The membrane localization of TRAF2 was confirmed using laser confocal light microscopy. **d** TRAF2 gene expression was silenced by siRNA, and both the protein and mRNA expression of TRAF2 were clearly downregulated. **e** The viability of hFLSs transfected with TRAF2 siRNA or the negative control was analyzed using MTT assays. **f** Intracellular cAMP levels were not decreased in TRAF2-silenced hFLSs, even after stimulation with TNF-α with or without INN. **g–j** Total and membrane EP4 expression was increased and cytoplasmic EP4 was decreased in hFLSs cultured with TNF-α with or without INN in the absence of TRAF2. **k** TRAF2 silencing decreased the gene expression of EP4 in hFLSs. Gene expression was quantified relative to the internal control (GAPDH). *$P < 0.05$, **$P < 0.01$ ($n = 6$).
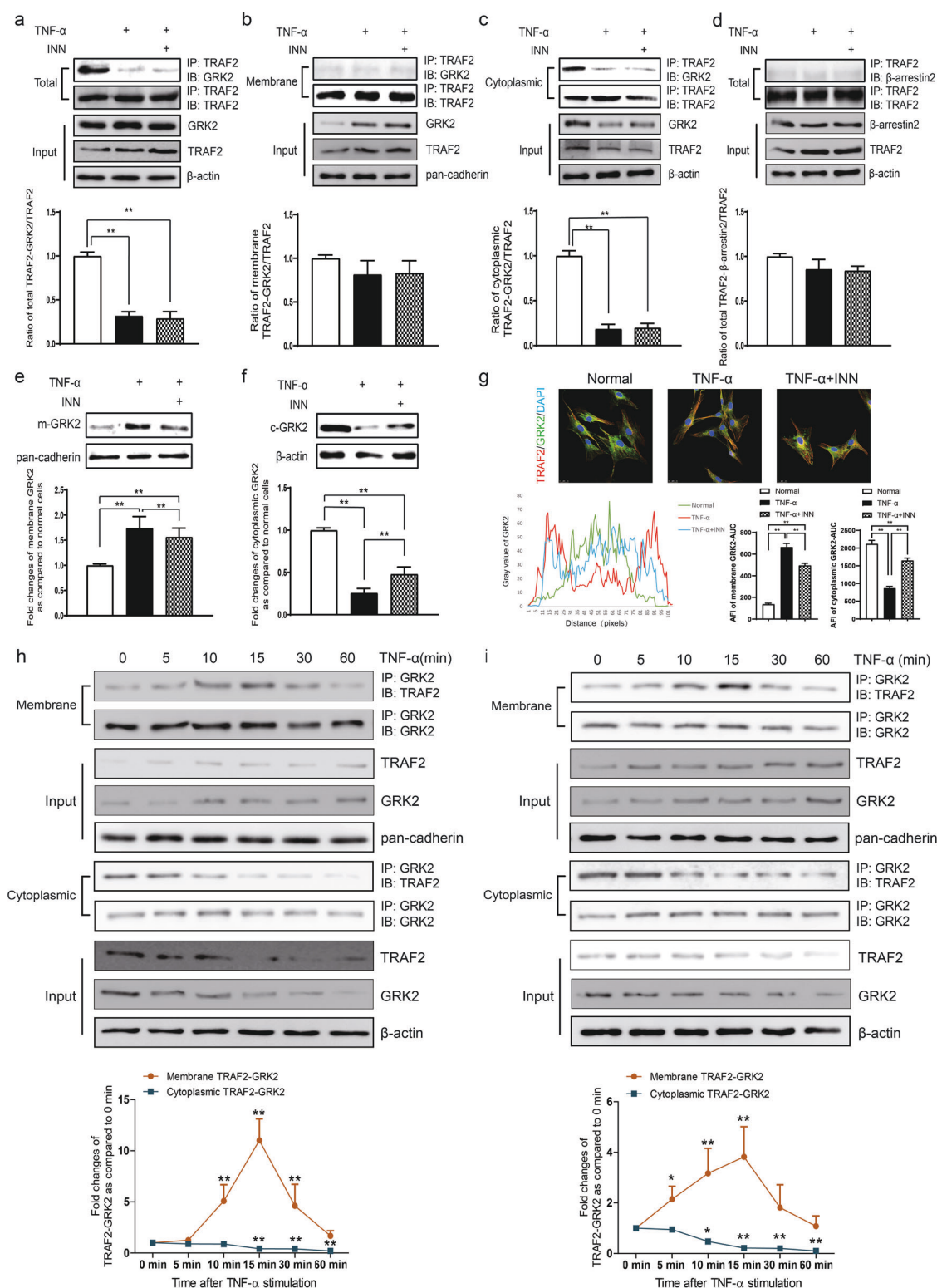
Fig. 4 TNF-α triggers the translocation of the TRAF2-GRK2 complex to the cell membrane and induces complex dissociation. a–d The subcellular localization of the TRAF2-GRK2/β-Arrestin2 complex was observed in purified hFLSs after stimulation with TNF-α with or without INN. **e, f** GRK2 translocation in response to both treatments was examined by Western blotting. **g** Laser confocal light microscopy was used to demonstrate the colocalization of TRAF2 and GRK2 in hFLSs. **h** Changes in the interaction between TRAF2 and GRK2 in the cell membrane and cytoplasm under TNF-α stimulation were determined via coimmunoprecipitation. **i** Synovial tissue was collected from the rat knee joint at different time points after local injection of 20 ng/mL TNF-α. The distribution of the TRAF2-GRK2 complex was analyzed. *$P < 0.05$, **$P < 0.01$ ($n = 6$).

a

b
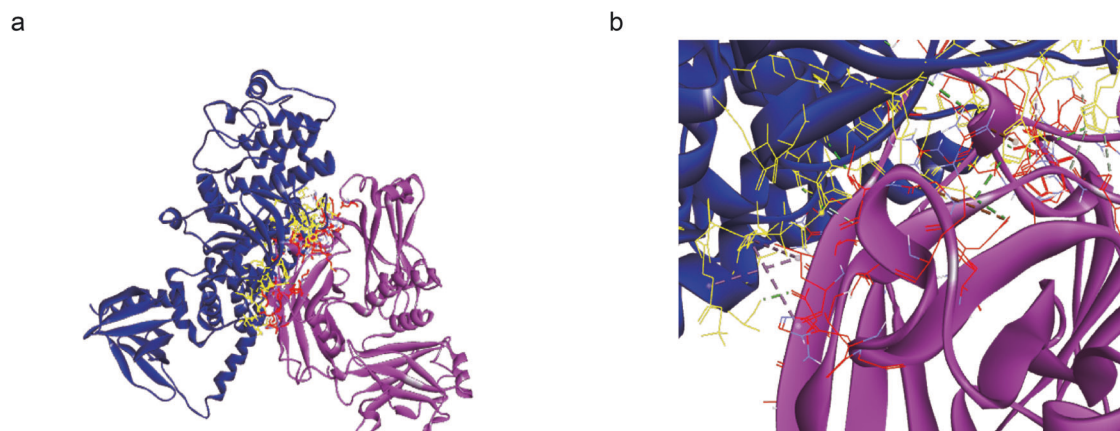
Fig. 5 Molecular docking of GRK2 and TRAF2. a Overall diagram of the GRK2 and TRAF2 docking results. Blue indicates the receptor GRK2, pink indicates the ligand TRAF2, red indicates interface ligand residues, and yellow indicates interface receptor residues. **b** Local plot of the TRAF2 and GRK2 docking results. The dashed line represents the existing interaction force between the ligand and receptor.

and then decreased. Less cytoplasmic TRAF2-GRK2 interactions were found in TNF-α-challenged rats than in saline-stimulated rats in a time-dependent manner, which was consistent with the in vitro results (Fig. 4i). To further identify the interaction between GRK2 and TRAF2, we used semiflexible small molecule and protein docking analysis on a DS platform. The target sequence of GRK2 was obtained from 3V5W alignment of the RCSB PDB database. GRK2 is composed of three different domains: an RGS homology (RH) domain, a protein kinase domain and a pleckstrin homology (PH) domain [32]. One feature of TRAF family members (except TRAF7) is the protein-protein interaction domain with ~230 amino acid residues at the C-terminus, which is known as the TRAF domain. The TRAF domain is subdivided into two different subdomains: the TRAF-N domain (a coiled-coil domain) and the TRAF-C domain (composed of 7 to 8 antiparallel β-chain folds). Members of the TRAF family form a mushroom-like trimeric structure in solution with TRAF domains, which is the functional unit of TRAF [33]. PDB ID: 1CA4 is the structure of the TRAF domain of human TRAF2. The best binding form with the lowest binding energy is presented in Fig. 5a, b.

TRAF2 promotes EP4 desensitization by activating GRK2 which contributes to hFLS proliferation
How is GRK2 recruited to the cell membrane in response to TNF-α stimulation? Analysis of the membrane and cytoplasmic protein levels of GRK2 in TRAF2-deficient hFLSs showed that membrane GRK2 was prominently decreased compared with that in the control siRNA group (Fig. 6a); conversely, cytoplasmic GRK2 was increased in both stimulation groups compared with that of hFLSs transfected with control siRNA (Fig. 6b). These results suggest that TNF-α modulates EP4-Gαs-cAMP signaling through the hetero-geneous TRAF2-GRK2 complex. Thus, the interaction between TRAF2 and GRK2 may play a pivotal role in the crosstalk between the TNF-α and EP4 signaling pathways. In addition, we concluded that TRAF2 binds with GRK2 and is mainly distributed in the cytoplasm of normal primary hFLSs. The complex dissociates upon TNF-α stimulation, and both TRAF2 and GRK2 simultaneously translocate to the cell membrane, resulting in desensitization and internalization of EP4. GRK2 fails to be recruited to the cell membrane in the absence of TRAF2, indicating that TRAF2 promotes GRK2 translocation in the presence of TNF-α. In addition, as shown in Fig. 6c, measurement of phospho-GRK2 in the hFLS membrane revealed that TRAF2 also contributes to the activation of GRK2. Paroxetine, a selective serotonin reuptake inhibitor, was found to inhibit GRK2 [34]. To verify the effect of GRK2 on TNF-α-induced hFLS proliferation, paroxetine was added. The results

suggest that inhibiting GRK2 attenuates TNF-α-induced hFLS proliferation (Fig. 6d).

Paroxetine treatment attenuated the symptoms of CIA rats
In FLSs from patients with RA, the concentration of cAMP was lower than that in primary hFLSs, while cell viability was enhanced (Fig. 7a, b). Accordingly, we investigated the relationship between the TNF-α-induced decrease in cAMP and the membrane expression of EP 1, 2, 3, and 4 in CIA FLSs by Western blotting. As shown in Fig. 7c, the uninjected hind paw appeared significantly swollen and enlarged on day 28. The cAMP concentration of CIA FLSs was lower than that of normal rat FLSs, and cell viability was enhanced (Fig. 7d, e). Body weight and pathological manifestations were observed every two days after the booster injection. CIA rats showed severe body weight loss, with significantly higher clinical manifestation scores, arthritis indexes, numbers of swollen joints and sizes of secondary paw swelling than control rats (Fig. 7f–j). MTX is a widely used RA treatment, and both paroxetine and MTX clearly exerted positive effects on alleviating the symptoms of CIA rats. Although there was no significant difference compared with that in the MTX group, paroxetine treatment restored the body weights of CIA rats. Regarding the alleviation of global symptoms in CIA rats, paroxetine exerted moderate therapeutic effects compared with those of MTX. Pathological changes in CIA joints were analyzed by H&E staining. Normal joints had only 1–3 layers of synoviocytes, and histological examination of CIA joints showed excessive synoviocyte proliferation and disorder, accompanied by a large amount of lymphocyte infiltration, abundant pannus formation, obvious cartilage erosion and evident local inflammation (Fig. 7k). As expected, MTX significantly reduced synovial inflammation and bone destruction in CIA joints. Paroxetine significantly prevented histological damage to the joints of CIA rats.

DISCUSSION
Proinflammatory cytokines such as TNF-α and PGE$_2$ participate in the regulation of inflammatory joint diseases, including RA. The high levels of TNF-α in the RA synovium play an important role in synovial hyperplasia in RA by suppressing apoptosis and promoting the proliferation of synoviocytes through NF-κB-dependent signaling pathways mediated by upregulated TNFR2 and TRAF2 [35]. TNF-α also stimulates synovial fibroblasts to secrete mediators such as PGE$_2$, matrix metalloproteinases (MMPs), and vascular endothelial growth factor (VEGF), which regulate inflammation, connective tissue degradation, and
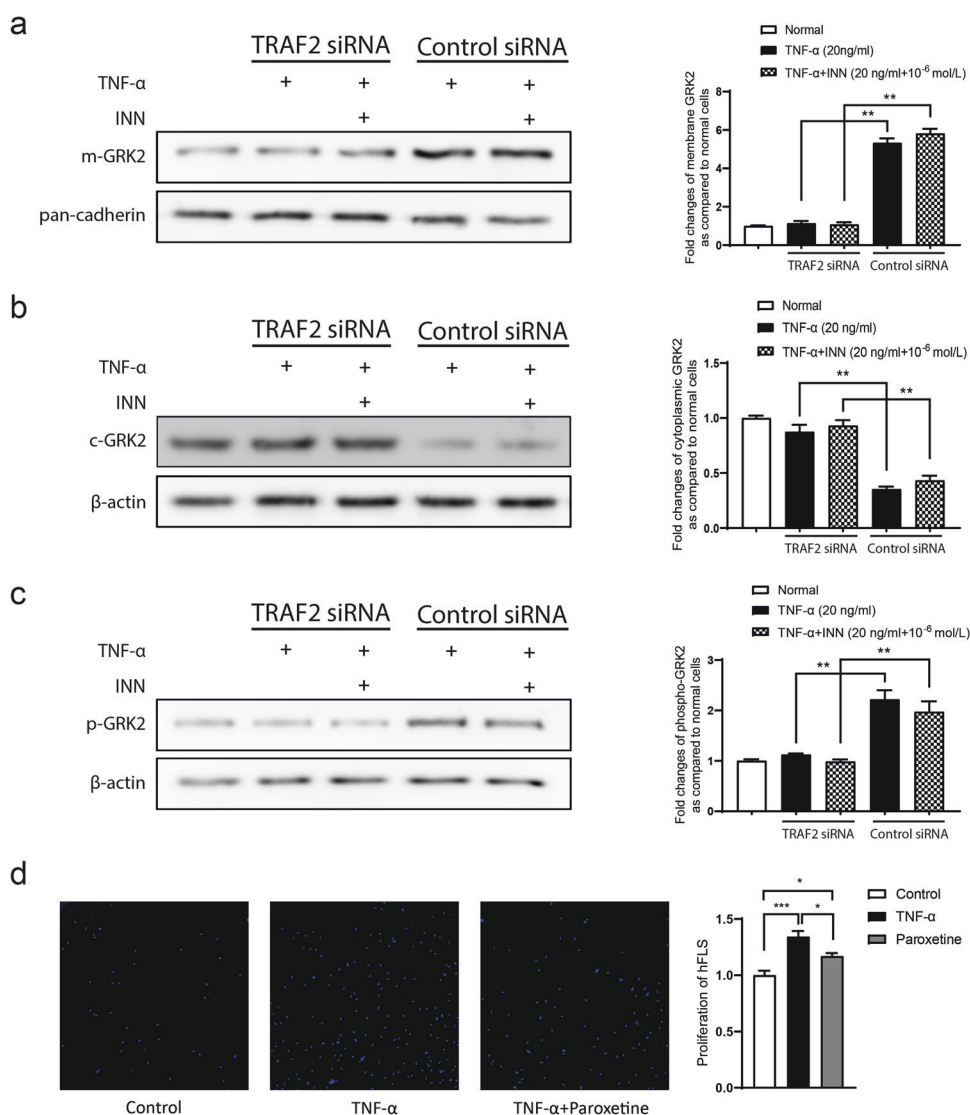
Fig. 6 TRAF2 silencing reduces EP4 desensitization by decreasing membrane GRK2 translocation. Inhibition of GRK2 attenuates TNF-α-induced FLS proliferation. a–c Membrane, cytoplasmic and phospho-GRK2 levels in hFLSs treated with TNF-α with or without INN were measured by Western blotting. **d** High-content screening was used to analyze hFLS proliferation after treatment with TNF-α with or without paroxetine (×100). *$P < 0.05$, **$P < 0.01$, ***$P < 0.001$ ($n = 6$).

angiogenesis, respectively [36]. Among these important proinflammatory factors in the RA synovial microenvironment, only PGE$_2$ receptors (EPs) are GPCRs [37]. Our previous experiments showed that TNF-α also plays a critical role in cAMP production. This information led us to hypothesize that TNF-α regulates GPCR signaling in hFLSs through downstream molecules. Therefore, in our present study, we screened the potential target GPCR of TNF-α in CIA FLSs. EP2 and EP4 were abundantly expressed in both CIA FLSs and normal hFLSs, which was consistent with other reported findings [38]. According to the correlation coefficient analysis, TNF-α stimulation induced EP4 internalization from the cell membrane, and this change directly decreased the cAMP concentration, which indicates that the reduction in cAMP in TNF-α-stimulated hFLSs is primarily due to EP4 desensitization and internalization. EP2 and EP4 often mediate similar effects, but responses to EP4 stimulation are typically more prominent [39].

We used normal hFLSs to examine the complex networks of proinflammatory cytokines in RA synovial fibroblasts, and hFLSs were stimulated with TNF-α with or without INN to examine the mechanism by which EP4 is regulated by TNF-α. Indometacin is a

nonselective inhibitor of cyclooxygenase (COX) 1 and 2 and inhibits the endogenous production of prostaglandins [40]. Our results indicated that TNF-α obviously promoted the proliferation of hFLSs in a manner dependent on the combined actions of TNF-α and TNF-α-induced PGE$_2$. The administration of INN eliminated the specific effects of PGE$_2$ on EPs, providing a better observation of the function of TNF-α. TNF-α induces hFLS hyperplasia by binding with TNFR2, which activates the transcription factor nuclear factor-κB (NF-κB) and c-Jun N-terminal kinase (JNK) [41]. The mechanisms mediating these activations depend on the recruitment of TRAFs to the intracellular region of the receptor [42, 43]. Recruitment of TRAF2 to plasma membrane lipid rafts is important for NF-κB signaling activation [31]. TRAF2 is currently the best-characterized TRAF family member [44] and plays a key role in the signal transduction of TNFR1 and TNFR2 [41]. Genetic evidence indicates that TRAF2 is necessary for the ubiquitination of receptor interacting protein 1 (RIP1), which then serves as a platform for the recruitment and stimulation of IκB kinase (IKK), leading to the activation of NF-κB [45]. NF-κB is highly activated in RA synovial fibroblasts (RASFs) [46] and lining cells, produces a
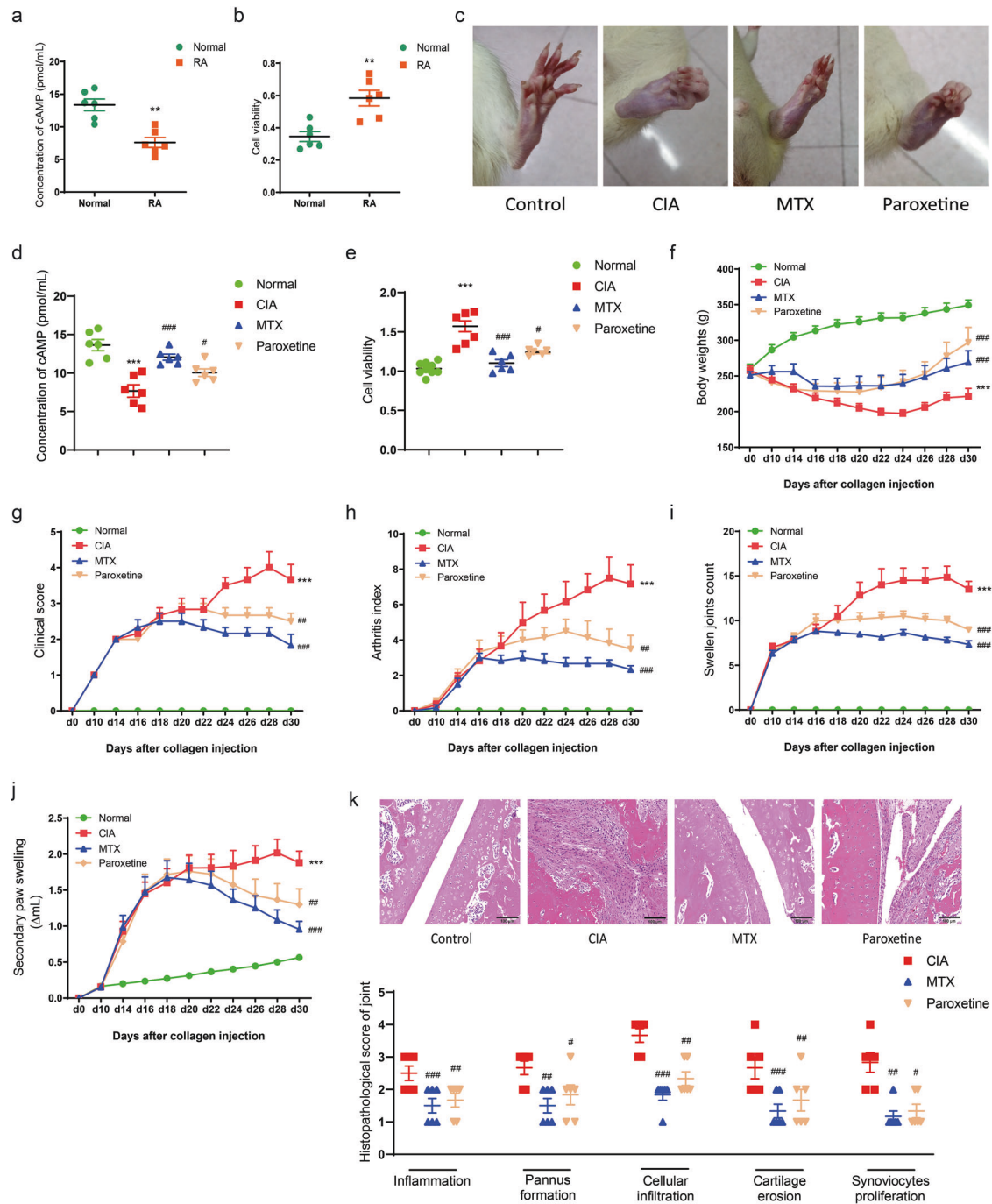
Fig. 7 Paroxetine treatment attenuates the symptoms of CIA rats. CIA was induced by immunizing rats with an emulsion of native chicken CII and incomplete Freund's adjuvant. **a**, **b** The concentration of intracellular cAMP and cell viability were compared between normal hFLSs and RA hFLSs. **c** The swelling of secondary joints reached a plateau on day 28. Obvious pathological changes were detected in the ankle joint. The degree of paw swelling was evaluated by the change in volume. **d**, **e** The concentration of cAMP and cell viability were analyzed in FLSs isolated from treated CIA rats. **f** Body weight. **g** Clinical score. **h** Arthritis index. **i** Swollen joint count. **j** Secondary paw swelling. **k** H&E staining of the joints was performed, and pathogenic parameters, including inflammation, pannus formation, cartilage erosion, cellular infiltration and synoviocyte proliferation, were evaluated (scale bar: 100 μm). $^{**}P < 0.01$, $^{***}P < 0.001$, vs the normal group; $^{#}P < 0.05$, $^{##}P < 0.01$, $^{###}P < 0.001$, vs the RA or CIA group ($n = 6$).

strong survival signal and links inflammation and a decrease in apoptosis [47] (Fig. 8). The membrane expression levels of TNFR2 and TRAF2 in hFLSs were obviously increased after TNF-α stimulation. Moreover, the expression of TRAF2 was significantly increased after the depletion of endogenous PGE$_2$ by INN. This finding suggests that TNF-α–induced PGE$_2$ production may

diminish TRAF2 expression, indicating that PGE$_2$ may play a considerable role in the TNF-α signaling pathway.

The data obtained in our study demonstrated that TRAF2 could negatively regulate EP4-Gαs-cAMP signaling by promoting the recruitment of GRK2 to the plasma membrane and GRK2 phosphorylation. TRAF2 associates with GRK2 in the cytoplasm
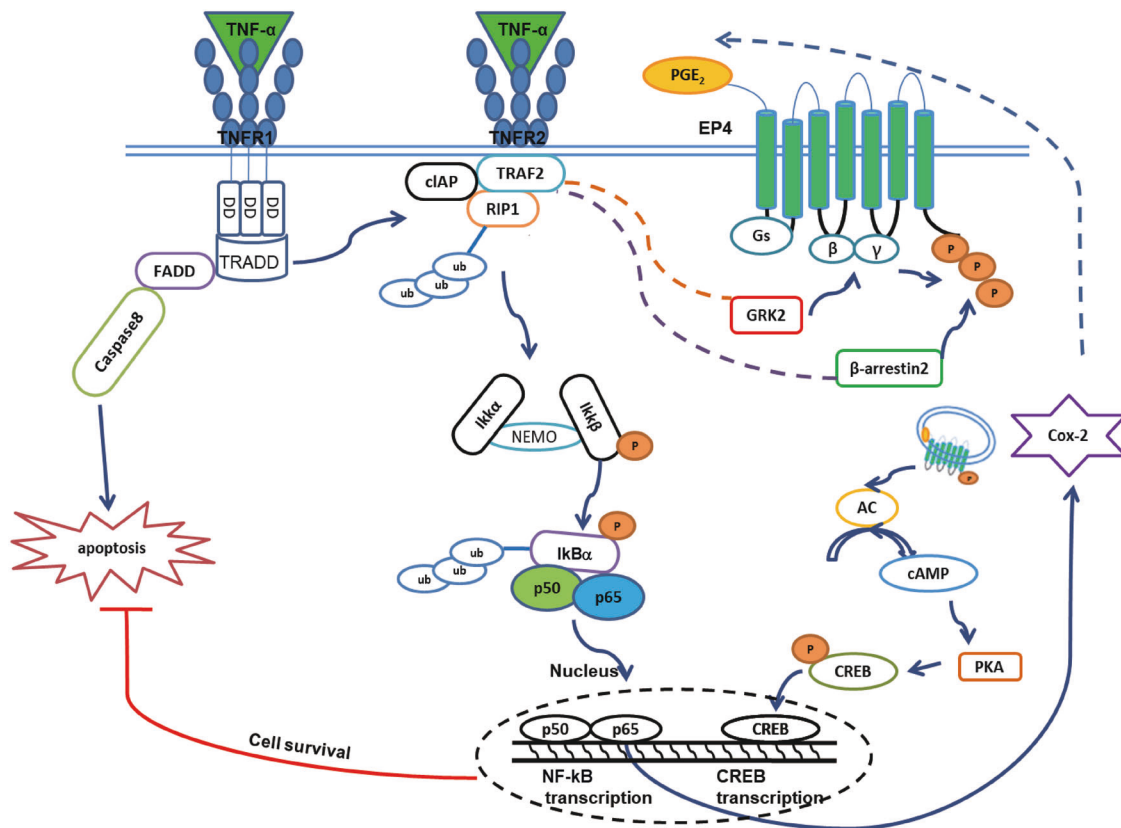
Fig. 8 Potential mechanisms of TNF-α-mediated EP4 signaling. Signaling pathways activated by TNF-α-induced PGE$_2$ stimulation of the human receptor EP4. EP4 is quickly phosphorylated by GRK2 and subjected to desensitization after agonist exposure. Then, β-Arrestin2 binds to phosphorylated EP4 and mediates its internalization. EP4 generates intracellular cAMP by coupling to Gs proteins, leading to the activation of PKA and CREB phosphorylation. TNF-α not only stimulates PGE$_2$ production but also interacts with GRK2 through TRAF2 to regulate EP4 desensitization in hFLSs

of normal hFLSs. In response to TNF-α, GRK2 is passively pulled to the cell membrane by the translocation of TRAF2 within 15 min, and GRK2 is then released and phosphorylated on the membrane, inducing excessive desensitization and internalization of EP4. The functional loss of EP4 attenuates the activation of Gαs and ultimately leads to a reduction in cAMP. cAMP inhibits cell growth by blocking growth factor activation of extracellular signal-related kinases (ERKs) [48]. The TNF-α-mediated reduction in cAMP production contributes to further proliferation and activation of hFLSs in a manner independent of the TNFR pathway, which indicates a new pattern of TNF-α actions in RA.

TNF blockers, such as etanercept, infliximab, adalimumab, and golimumab, suppress the immune system by interfering with the effects of TNF-α and have been shown to be highly effective in treating RA. However, increased frequencies of infection, cancer and neurological side effects have been reported during TNF therapy [49]. TNF-α can not only cause inflammation but also plays an important role in host defense, particularly in the killing of intracellular microorganisms such as Listeria and Mycobacteria and in inducing apoptosis in some tumor cells [50]. Consequently, there has been some concern that long-term inhibition of TNF is not a medically satisfying approach for RA treatment [51]. Specifically, attenuating TNF-α activation and blocking crosstalk with other stimulatory signals may be a potent therapeutic strategy.

GRK2 is a family of protein kinases that regulates the activity of GPCRs by phosphorylating their intracellular domains after the associated G proteins have been released and activated. Many studies have been elucidated the function of GRK2 in regulating EPs [52–54]. Shi and colleagues reported that similar to GRK2, the

kinases apoptosis signal-regulating kinase 1 (ASK1) and germinal center kinase (GCK) can bind with the TRAF domain of TRAF2, and the RING finger domain is needed for their activation [55]. The TRAF2-binding region of ASK1 is the amino- and carboxyl-terminal noncatalytic domain [56]. Other researchers have shown that NF-κB-inducing kinase (NIK) association with TRAF2 requires the conserved WKI motif within the TRAF domain and mediates TNF activation of NF-κB [57]. This evidence could provide clues to map the binding domain regions of TRAF2 and GRK2.

TNFR1 contains a death domain in its intracellular region, but TNFR2 does not [58]. Activation of TNFR1 induces the formation of two different TNF receptor signaling complexes. Complex I controls the expression of antiapoptotic proteins that prevent activation of cell death processes, whereas Complex II triggers cell death processes [59]. We noted that silencing TRAF2 using siRNA caused significant increases in cAMP levels. This result is consistent with the changes in hFLS proliferation induced by TRAF2 siRNA. After TRAF2 knockdown, the TNF-α plus INN group almost completely lost the ability to promote hFLS proliferation. TRAF2 deficiency did not significantly affect the TNF-α-induced generation of PGE$_2$ in hFLSs.

GPCR functions are precisely controlled by G protein-coupled receptor kinases (GRKs) and β-arrestins. GPCR desensitization is triggered by the GRK-mediated phosphorylation of ligand-activated GPCRs within the third intracellular loop or carboxy-terminal tail [60]. GRKs include seven known subtypes (GRK1-GRK 7), of which four members, GRK2, -3, -5, and -6, are ubiquitously expressed [61]. In particular, GRK2 and GRK6 are involved in the abnormal proliferation of FLSs in RA models [62, 63]. In our study, to determine the mechanism by which TNF-α promotes EP4

desensitization, we assessed whether TRAF2 interacts with GRK2/β-arrestin2 in hFLSs. The results showed that TRAF2 could interact with both GRK2 and β-arrestin2 in hFLSs. Interestingly, we further found that TRAF2 interacts with GRK2 to prevent it from participating in the regulation of EP4 receptor desensitization under normal conditions. However, in response to TNF-α with or without INN, the ability of TRAF2 to interact with GRK2 was weakened, which indicated that the dissociation of GRK2 was increased. Then, EP4 desensitization was increased, and the relatively high intracellular levels of EP4 in hFLSs inhibited cAMP production and promoted cell survival. This is the first study to show the interaction between TRAF2 and GRK2, and TRAF2 can regulate the desensitization of EP4 through GRK2 under TNF-α stimulation.

To better understand this apparent shift in EP4 function, we carried out the next experiment. The TRAF2-GRK2 interaction was weakened after transfection with TRAF2 siRNA. Logically, the dissociation of GRK2 was greatly increased. However, the membrane level of EP4 was elevated. To further confirm these results, we found that membrane GRK2 was prominently decreased and cytoplasmic GRK2 was significantly increased after transfection with TRAF2 siRNA. These results suggested that TRAF2 could promote GRK2 translocation, but the mechanism by which TRAF2 controls the translocation of GRK2 to the plasma membrane remains unknown. Multiple mechanisms have been shown to regulate the association of GRK2 with the plasma membrane and GRK2 activity, including the regulation of GRK2 by other kinases, such as PKA, PKC, and MAPKs, during the activation of GPCRs [64]. An alternative explanation is that the increased activity and membrane availability of GRK2 in TNF-α-stimulated cells during GPCR activation may result from decreased binding of other cytosolic inhibitor proteins to GRK2 or increased binding of GRK2 to other cytosolic proteins to promote GRK2 activity. Another possible explanation is that the binding region of these two molecules is important for GRK2 activity and translocation, and these hypotheses need to be further investigated. In the future, we will determine (a) the structural domain responsible for the interaction between TRAF2 and GRK2 and (b) whether TRAF2 directly or indirectly modulates the translocation of GRK2.

According to the study results, TNF-α triggers the translocation of the TRAF2-GRK2 complex to the cell membrane, and GRK2 on the cell membrane may desensitize EP4, resulting in a reduction in cAMP levels. This TNF-α-TRAF2-GRK2-EP4 signaling pathway is involved in synoviocyte hyperplasia. TRAF2 and GRK2 are key factors in this mechanism and can be used as therapeutic targets for treating RA. However, no TRAF2 inhibitor is currently available, and so we used a GRK2 inhibitor to block this pathway and investigated its effect in treating arthritic animals. Paroxetine is a classic drug for treating depression and has been confirmed to have strong GRK2 inhibitory effects. Therefore, we used paroxetine to inhibit GRK2 to study whether GRK2 inhibitors could abrogate the reduction in cAMP in TNF-α-stimulated hFLSs, thereby effectively preventing the proliferation of inflammatory synovial cells. This experiment further verified the pathological role of the TNF-α-TRAF2-GRK2-EP4 signaling pathway in the abnormal proliferation of hFLSs. Due to the potential side effects in the central nervous system, paroxetine is not suitable for treating RA in the clinic. Because of the important role of GRK2 in many diseases, several GRK2 inhibitors with relatively mild side effects are undergoing preclinical research. MTX, a dihydrofolate reductase inhibitor, is a commonly used drug for treating RA. Our data showed that MTX effectively improved the clinical parameters of CIA rats and was even slightly better than paroxetine, but no significant differences between the two drugs were observed. According to the American Rheumatology Association, the effective rate of MTX in treating RA and animal models is less than 50%, and some patients give up treatment because of the severe side effects [65]. Therefore, the development of new

therapeutic targets and new drugs for RA therapy is urgent. GRK2 is a promising target for the development of new antirheumatic therapies.

In this study on hFLSs, we determined that TNF-α affected the desensitization of EP4 and examined the effect of TNF-α on the expression and subcellular distribution of GRK2. These findings suggested that TRAF2 not only terminated TNF-α signaling but also regulated the GPCR signaling pathway by binding to GRK2 to control the dissociation of GRK2 from the membrane and then promoted the TNF-α-induced proliferation of hFLSs via the EP4-AC-cAMP pathway.

AUTHOR CONTRIBUTIONS
YT, BH, PPG, ZW, ZWZ, MMW, HFS, YH, SLX and LLZ conducted the study and analyzed the data, YT, QTW and WW analyzed the data and wrote the paper.

ADDITIONAL INFORMATION
Competing interests: The authors declare no competing interests.

REFERENCES
1. Dayer JM. From supernatants to cytokines: a personal view on the early history of IL-1, IL-1Ra, TNF and its inhibitor in rheumatology. Arthritis Res Ther. 2018;20:101.
2. Ursini F, Leporini C, Bene F, D'Angelo S, Mauro D, Russo E, et al. Anti-TNF-alpha agents and endothelial function in rheumatoid arthritis: a systematic review and meta-analysis. Sci Rep. 2017;7:5346.
3. Jia XY, Chang Y, Sun XJ, Dai X, Wei W. The role of prostaglandin E2 receptor signaling of dendritic cells in rheumatoid arthritis. Int Immunopharmacol. 2014;23:163–9.
4. Samuels JS, Holland L, Lopez M, Meyers K, Cumbie WG, McClain A, et al. Prostaglandin E2 and IL-23 interconnects STAT3 and RoRgamma pathways to initiate Th17 CD4$^+$ T-cell development during rheumatoid arthritis. Inflamm Res. 2018;67:589–96.
5. Lowin T, Apitz M, Anders S, Straub RH. Anti-inflammatory effects of N-acylethanolamines in rheumatoid arthritis synovial cells are mediated by TRPV1 and TRPA1 in a COX-2 dependent manner. Arthritis Res Ther. 2015;17:321.
6. Li H, Chen HY, Liu WX, Jia XX, Zhang JG, Ma CL, et al. Prostaglandin E2 restrains human Treg cell differentiation via E prostanoid receptor 2-protein kinase A signaling. Immunol Lett. 2017;191:63–72.
7. Frolov A, Yang L, Dong H, Hammock BD, Crofford LJ. Anti-inflammatory properties of prostaglandin E2: deletion of microsomal prostaglandin E synthase-1 exacerbates non-immune inflammatory arthritis in mice. Prostaglandins Leukot Ess Fat Acids. 2013;89:351–8.
8. Shibata-Nozaki T, Ito H, Mitomi H, Akaogi J, Komagata T, Kanaji T, et al. Endogenous prostaglandin E2 inhibits aberrant overgrowth of rheumatoid synovial tissue and the development of osteoclast activity through EP4 receptor. Arthritis Rheum. 2011;63:2595–605.
9. Treutlein EM, Kern K, Weigert A, Tarighi N, Schuh CD, Nusing RM, et al. The prostaglandin E2 receptor EP3 controls CC-chemokine ligand 2-mediated neuropathic pain induced by mechanical nerve damage. J Biol Chem. 2018;293:9685–95.
10. Kawashima M, Ogura N, Akutsu M, Ito K, Kondoh T. The anti-inflammatory effect of cyclooxygenase inhibitors in fibroblast-like synoviocytes from the human temporomandibular joint results from the suppression of PGE2 production. J Oral Pathol Med. 2013;42:499–506.
11. Vitali E, Cambiaghi V, Spada A, Tresoldi A, Zerbi A, Peverelli E, et al. cAMP effects in neuroendocrine tumors: The role of Epac and PKA in cell proliferation and adhesion. Exp Cell Res. 2015;339:241–51.

12. Liu D, Huang Y, Bu D, Liu AD, Holmberg L, Jia Y, et al. Sulfur dioxide inhibits vascular smooth muscle cell proliferation via suppressing the Erk/MAP kinase pathway mediated by cAMP/PKA signaling. Cell Death Dis. 2014;5:e1251.

13. Uemura Y, Shibata R, Ohashi K, Enomoto T, Kambara T, Yamamoto T, et al. Adipose-derived factor CTRP9 attenuates vascular smooth muscle cell proliferation and neointimal formation. FASEB J. 2013;27:25–33.

14. Xie J, Ponuwei GA, Moore CE, Willars GB, Tee AR, Herbert TP. cAMP inhibits mammalian target of rapamycin complex-1 and -2 (mTORC1 and 2) by promoting complex dissociation and inhibiting mTOR kinase activity. Cell Signal. 2011;23:1927–35.

15. Sun L, Zhao R, Zhang L, Zhang W, He G, Yang S, et al. Prevention of vascular smooth muscle cell proliferation and injury-induced neointimal hyperplasia by CREB-mediated p21 induction: an insight from a plant polyphenol. Biochem Pharmacol. 2016;103:40–52.

16. Park ES, Choi S, Shin B, Yu J, Yu J, Hwang JM, et al. Tumor necrosis factor (TNF) receptor-associated factor (TRAF)-interacting protein (TRIP) negatively regulates the TRAF2 ubiquitin-dependent pathway by suppressing the TRAF2-sphingosine 1-phosphate (S1P) interaction. J Biol Chem. 2015;290:9660–73.

17. Chang Y, Wei W, Zhang L, Xu HM. Effects and mechanisms of total glucosides of paeony on synoviocytes activities in rat collagen-induced arthritis. J Ethnopharmacol. 2009;121:43–8.

18. Wang QT, Zhang LL, Wu HX, Wei W. The expression change of beta-arrestins in fibroblast-like synoviocytes from rats with collagen-induced arthritis and the effect of total glucosides of paeony. J Ethnopharmacol. 2011;133:511–6.

19. Huang B, Wang QT, Song SS, Wu YJ, Ma YK, Zhang LL, et al. Combined use of etanercept and MTX restores CD4$^+$/CD8$^+$ ratio and Tregs in spleen and thymus in collagen-induced arthritis. Inflamm Res. 2012;61:1229–39.

20. Nair A, Kanda V, Bush-Joseph C, Verma N, Chubinskaya S, Mikecz K, et al. Synovial fluid from patients with early osteoarthritis modulates fibroblast-like synoviocyte responses to toll-like receptor 4 and toll-like receptor 2 ligands via soluble CD14. Arthritis Rheum. 2012;64:2268–77.

21. Lane JR, Beukers MW, Mulder-Krieger T, Ijzerman AP. The endocannabinoid 2-arachidonylglycerol is a negative allosteric modulator of the human A3 adenosine receptor. Biochem Pharmacol. 2010;79:48–56.

22. Sun Z, Runne C, Tang X, Lin F, Chen S. The Gbeta3 splice variant associated with the C825T gene polymorphism is an unstable and functionally inactive protein. Cell Signal. 2012;24:2349–59.

23. Han YS, Lan L, Chu J, Kang WQ, Ge ZM. Epigallocatechin gallate attenuated the activation of rat cardiac fibroblasts induced by angiotensin II via regulating beta-arrestin1. Cell Physiol Biochem. 2013;31:338–46.

24. Isono E, Schwechheimer C. Co-immunoprecipitation and protein blots. Methods Mol Biol. 2010;655:377–87.

25. Huang C, Dai X, Chai W. Human Stn1 protects telomere integrity by promoting efficient lagging-strand synthesis at telomeres and mediating C-strand fill-in. Cell Res. 2012;22:1681–95.

26. Foudi N, Kotelevets L, Louedec L, Leseche G, Henin D, Chastre E, et al. Vasorelaxation induced by prostaglandin E2 in human pulmonary vein: role of the EP4 receptor subtype. Br J Pharmacol. 2008;154:1631–9.

27. Angiolilli C, Kabala PA, Grabiec AM, Rossato M, Lai WS, Fossati G, et al. Control of cytokine mRNA degradation by the histone deacetylase inhibitor ITF2357 in rheumatoid arthritis fibroblast-like synoviocytes: beyond transcriptional regulation. Arthritis Res Ther. 2018;20:148.

28. Wang H, Dong BW, Zheng ZH, Wu ZB, Li W, Ding J. Metastasis-associated protein 1 (MTA1) signaling in rheumatoid synovium: regulation of inflammatory response and cytokine-mediated production of prostaglandin E2 (PGE2). Biochem Biophys Res Commun. 2016;473:442–8.

29. Quistad SD, Traylor-Knowles N. Precambrian origins of the TNFR superfamily. Cell Death Discov. 2016;2:16058.

30. Cabal-Hierro L, Lazo PS. Signal transduction by tumor necrosis factor receptors. Cell Signal. 2012;24:1297–305.

31. Legler DF, Micheau O, Doucey MA, Tschopp J, Bron C. Recruitment of TNF receptor 1 to lipid rafts is essential for TNFalpha-mediated NF-kappaB activation. Immunity. 2003;18:655–64.

32. Lodowski DT, Barnhill JF, Pyskadlo RM, Ghirlando R, Sterne-Marr R, Tesmer JJ. The role of G beta gamma and domain interfaces in the activation of G protein-coupled receptor kinase 2. Biochemistry. 2005;44:6958–70.

33. Park HH. Structure of TRAF family: current understanding of receptor recognition. Front Immunol. 2018;9:1999.

34. Schumacher SM, Gao E, Zhu W, Chen X, Chuprun JK, Feldman AM, et al. Paroxetine-mediated GRK2 inhibition reverses cardiac dysfunction and remodeling after myocardial infarction. Sci Transl Med. 2015;7:277ra231.

35. Stork PJ, Schmitt JM. Crosstalk between cAMP and MAP kinase signaling in the regulation of cell proliferation. Trends Cell Biol. 2002;12:258–66.

36. Youn J, Kim HY, Park JH, Hwang SH, Lee SY, Cho CS, et al. Regulation of TNF-alpha-mediated hyperplasia through TNF receptors, TRAFs, and NF-kappaB in synoviocytes obtained from patients with rheumatoid arthritis. Immunol Lett. 2002;83:85–93.

37. De Keijzer S, Meddens MB, Torensma R, Cambi A. The multiple faces of prostaglandin E2 G-protein coupled receptor signaling during the dendritic cell life cycle. Int J Mol Sci. 2013;14:6542–55.

38. Kunisch E, Jansen A, Kojima F, Loffler I, Kapoor M, Kawai S, et al. Prostaglandin E2 differentially modulates proinflammatory/prodestructive effects of TNF-alpha on synovial fibroblasts via specific E prostanoid receptors/cAMP. J Immunol. 2009;183:1328–36.

39. Woodward DF, Jones RL, Narumiya S. International Union of Basic and Clinical Pharmacology. LXXXIII: classification of prostanoid receptors, updating 15 years of progress. Pharmacol Rev. 2011;63:471–538.

40. Axelsson H, Lonnroth C, Andersson M, Lundholm K. Mechanisms behind COX-1 and COX-2 inhibition of tumor growth in vivo. Int J Oncol. 2010;37:1143–52.

41. Lin WJ, Su YW, Lu YC, Hao Z, Chio II, Chen NJ, et al. Crucial role for TNF receptor-associated factor 2 (TRAF2) in regulating NFkappaB2 signaling that contributes to autoimmunity. Proc Natl Acad Sci USA. 2011;108:18354–9.

42. Crunkhorn S. Inflammatory disorders: targeting TRAFs tames inflammation. Nat Rev Drug Discov. 2013;12:423.

43. Rodriguez M, Cabal-Hierro L, Carcedo MT, Iglesias JM, Artime N, Darnay BG, et al. NF-kappaB signal triggering and termination by tumor necrosis factor receptor 2. J Biol Chem. 2011;286:22814–24.

44. Kim S, Lewis C, Nadel JA. Epidermal growth factor receptor reactivation induced by E-prostanoid-3 receptor- and tumor necrosis factor-alpha-converting enzyme-dependent feedback exaggerates interleukin-8 production in airway cancer (NCI-H292) cells. Exp Cell Res. 2011;317:2650–60.

45. Alvarez SE, Harikumar KB, Hait NC, Allegood J, Strub GM, Kim EY, et al. Sphingosine-1-phosphate is a missing cofactor for the E3 ubiquitin ligase TRAF2. Nature. 2010;465:1084–8.

46. Niedermeier M, Pap T, Korb A. Therapeutic opportunities in fibroblasts in inflammatory arthritis. Best Pr Res Clin Rheumatol. 2010;24:527–40.

47. Bartok B, Firestein GS. Fibroblast-like synoviocytes: key effector cells in rheumatoid arthritis. Immunol Rev. 2010;233:233–55.

48. Doherty GA, Byrne SM, Molloy ES, Malhotra V, Austin SC, Kay EW, et al. Proneoplastic effects of PGE2 mediated by EP4 receptor in colorectal cancer. BMC Cancer. 2009;9:207.

49. Murdaca G, Colombo BM, Cagnati P, Gulli R, Spano F, Puppo F. Update upon efficacy and safety of TNF-alpha inhibitors. Expert Opin Drug Saf. 2012;11:1–5.

50. Ehlers S. Role of tumour necrosis factor (TNF) in host defence against tuberculosis: implications for immunotherapies targeting TNF. Ann Rheum Dis. 2003;62 (Suppl 2):ii37–42.

51. Canete JD, Pablos JL. Biologic therapy in rheumatoid arthritis. Curr Top Med Chem. 2013;13:752–9.

52. Eijkelkamp N, Wang H, Garza-Carbajal A, Willemen HL, Zwartkruis FJ, Wood JN, et al. Low nociceptor GRK2 prolongs prostaglandin E2 hyperalgesia via biased cAMP signaling to Epac/Rap1, protein kinase Cepsilon, and MEK/ERK. J Neurosci. 2010;30:12806–15.

53. Nichols HL, Saffeddine M, Theriot BS, Hegde A, Polley D, El-Mays T, et al. beta-Arrestin-2 mediates the proinflammatory effects of proteinase-activated receptor-2 in the airway. Proc Natl Acad Sci USA. 2012;109:16660–5.

54. Penn RB, Pascual RM, Kim YM, Mundell SJ, Krymskaya VP, Panettieri RA Jr., et al. Arrestin specificity for G protein-coupled receptors in human airway smooth muscle. J Biol Chem. 2001;276:32648–56.

55. Shi CS, Kehrl JH. Tumor necrosis factor (TNF)-induced germinal center kinase-related (GCKR) and stress-activated protein kinase (SAPK) activation depends upon the E2/E3 complex Ubc13-Uev1A/TNF receptor-associated factor 2 (TRAF2). J Biol Chem. 2003;278:15429–34.

56. Liu H, Nishitoh H, Ichijo H, Kyriakis JM. Activation of apoptosis signal-regulating kinase 1 (ASK1) by tumor necrosis factor receptor-associated factor 2 requires prior dissociation of the ASK1 inhibitor thioredoxin. Mol Cell Biol. 2000;20:2198–208.

57. Kalsoom UE, Habib R, Khan B, Ali G, Ali N, Ansar M, et al. Mutations in lipase H gene underlie autosomal recessive hypotrichosis in five Pakistani families. Acta Derm Venereol. 2010;90:93–4.

58. Ke F, Zhang L, Liu Z, Yan S, Xu Z, Bai J, et al. Soluble tumor necrosis factor receptor 1 released by skin-derived mesenchymal stem cells is critical for inhibiting Th17 cell differentiation. Stem Cells Transl Med. 2016;5:301–13.

59. Wheeler MA, Heffner DL, Kim S, Espy SM, Spano AJ, Cleland CL, et al. TNF-alpha/TNFR1 signaling is required for the development and function of primary nociceptors. Neuron. 2014;82:587–602.

60. Evron T, Daigle TL, Caron MG. GRK2: multiple roles beyond G protein-coupled receptor desensitization. Trends Pharmacol Sci. 2012;33:154–64.

61. Vroon A, Heijnen CJ, Kavelaars A. GRKs and arrestins: regulators of migration and inflammation. J Leukoc Biol. 2006;80:1214–21.

62. Chen JY, Wu HX, Chen Y, Zhang LL, Wang QT, Sun WY, et al. Paeoniflorin inhibits proliferation of fibroblast-like synoviocytes through suppressing G-protein-coupled receptor kinase 2. Planta Med. 2012;78:665–71.

63. Tarrant TK, Rampersad RR, Esserman D, Rothlein LR, Liu P, Premont RT, et al. Granulocyte chemotaxis and disease expression are differentially regulated by GRK subtype in an acute inflammatory arthritis model (K/BxN). Clin Immunol. 2008;129:115–22.

64. Ribas C, Penela P, Murga C, Salcedo A, Garcia-Hoz C, Jurado-Pueyo M, et al. The G protein-coupled receptor kinase (GRK) interactome: role of GRKs in GPCR regulation and signaling. Biochim Biophys Acta. 2007;1768:913–22.

65. Khanna D, Park GS, Paulus HE, Simpson KM, Elashoff D, Cohen SB, et al. Reduction of the efficacy of methotrexate by the use of folic acid: post hoc analysis from two randomized controlled studies. Arthritis Rheum. 2005;52:3030–8.